Electronic Supplementary Material (ESI) for Environmental Science: Nano.

Supporting Information for

Facet-dependent evolution of surface defects in anatase TiO_2 by thermal treatment: implications for environmental applications of photocatalysis

Tong Li [a], Zelin Shen [a], Yiling Shu [a], Xuguang Li [a, b], Chuanjia Jiang [a, *], Wei Chen [a, *]

[a] College of Environmental Science and Engineering, Ministry of Education Key Laboratory of Pollution Processes and Environmental Criteria, Tianjin Key Laboratory of Environmental Remediation and Pollution Control, Nankai University, Tianjin 300350, China

[b] School of Water Conservancy and Environment, University of Jinan, Jinan, Shandong 250022, China

* Corresponding authors: Chuanjia Jiang (E-mail: jiangcj@nankai.edu.cn); Wei Chen (Tel/Fax: + 86 22 66229516; E-mail: chenwei@nankai.edu.cn).

Table S1. The area ratio of the Raman vibrational modes

Material	The ratio of A_{1g}/E_g	The ratio of B_{1g}/E_g
{101}_P	0.058	0.047
{101}_Air	0.057	0.047
{101}_Ar	0.057	0.049
{010}_P	0.036	0.039
{010}_Air	0.037	0.040
{010}_Ar	0.036	0.039

[a] Analyzed by Raman spectroscopy. The Raman vibrational modes between E_g (140 cm^{-1}) and A_{1g} (515 cm^{-1})、B_{1g} (395 cm^{-1})

Table S2. Pseudo-first-order reaction rate constants (k_1) for photocatalytic degradation of BPA, Cr(VI), and RhB by different TiO_2 materials

Material	k_1 (min^{-1})			Surface area normalized k_1 ($min^{-1} \cdot m^{-2}$)		
	BPA	Cr(VI)	RhB	BPA	Cr(VI)	RhB
{101}_P	0.0761	0.0103	0.0420	5.44×10^{-3}	7.36×10^{-4}	3.00×10^{-3}
{101}_Air	0.0684	0.0096	0.0354	4.75×10^{-3}	6.67×10^{-4}	2.46×10^{-3}
{101}_Ar	0.0885	0.0111	0.0466	5.94×10^{-3}	7.45×10^{-4}	3.12×10^{-3}
{010}_P	0.0746	0.0222	0.0295	2.25×10^{-3}	6.69×10^{-4}	0.89×10^{-3}
{010}_Air	0.0897	0.0241	0.0383	2.89×10^{-3}	7.77×10^{-4}	1.23×10^{-3}
{010}_Ar	0.1018	0.0247	0.0450	3.19×10^{-3}	7.74×10^{-4}	1.41×10^{-3}

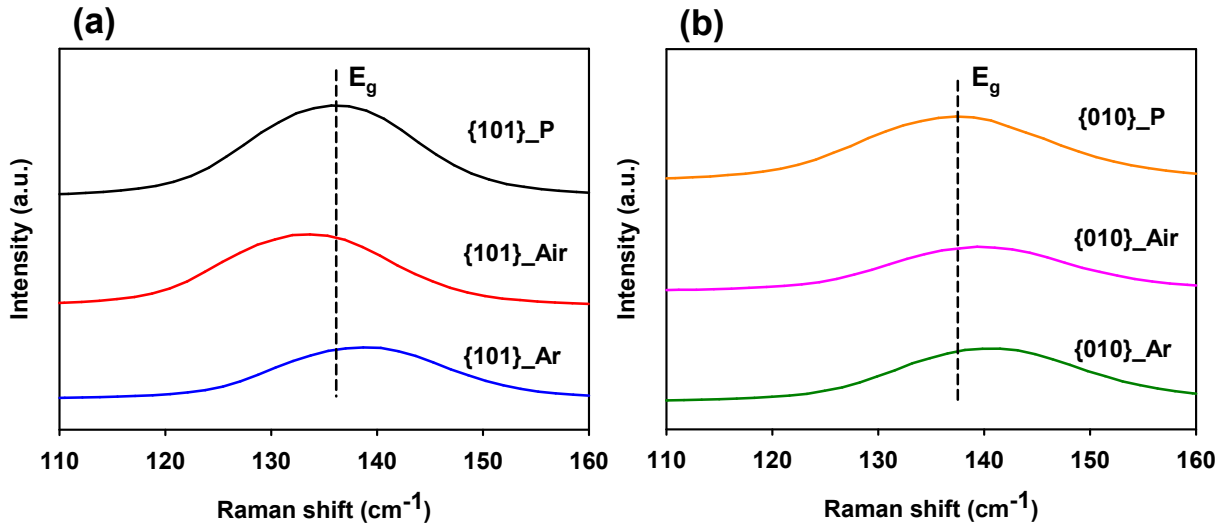

Fig. S1. The zoom-in views for Raman spectra of TiO_2 materials with predominantly exposed {101} facets (a) and {010} facets (b).

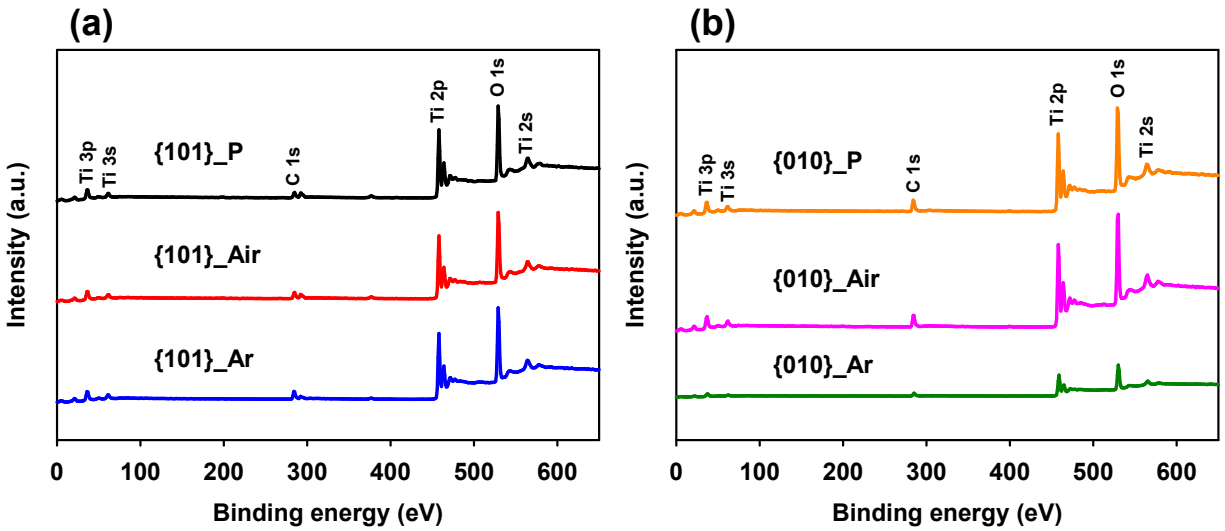

Fig. S2. XPS survey spectra of the TiO_2 materials with predominantly exposed {101} facets (a) and {010} facets (b).

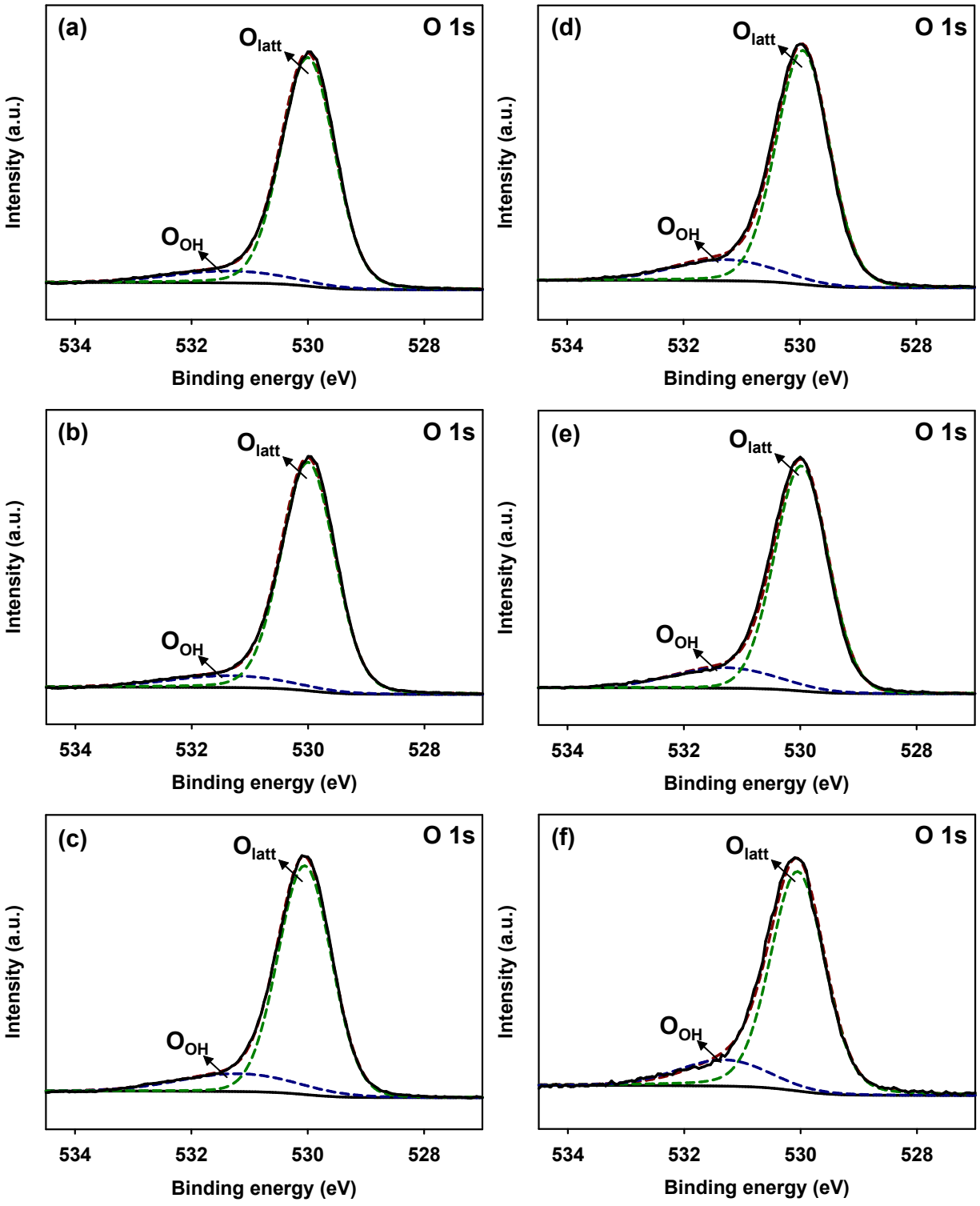

Fig. S3. High-resolution O 1s XPS spectra of {101}_P (a), {101}_Air (b), {101}_Ar (c), {010}_P (d), {010}_Air (e), {010}_Ar (f) materials.

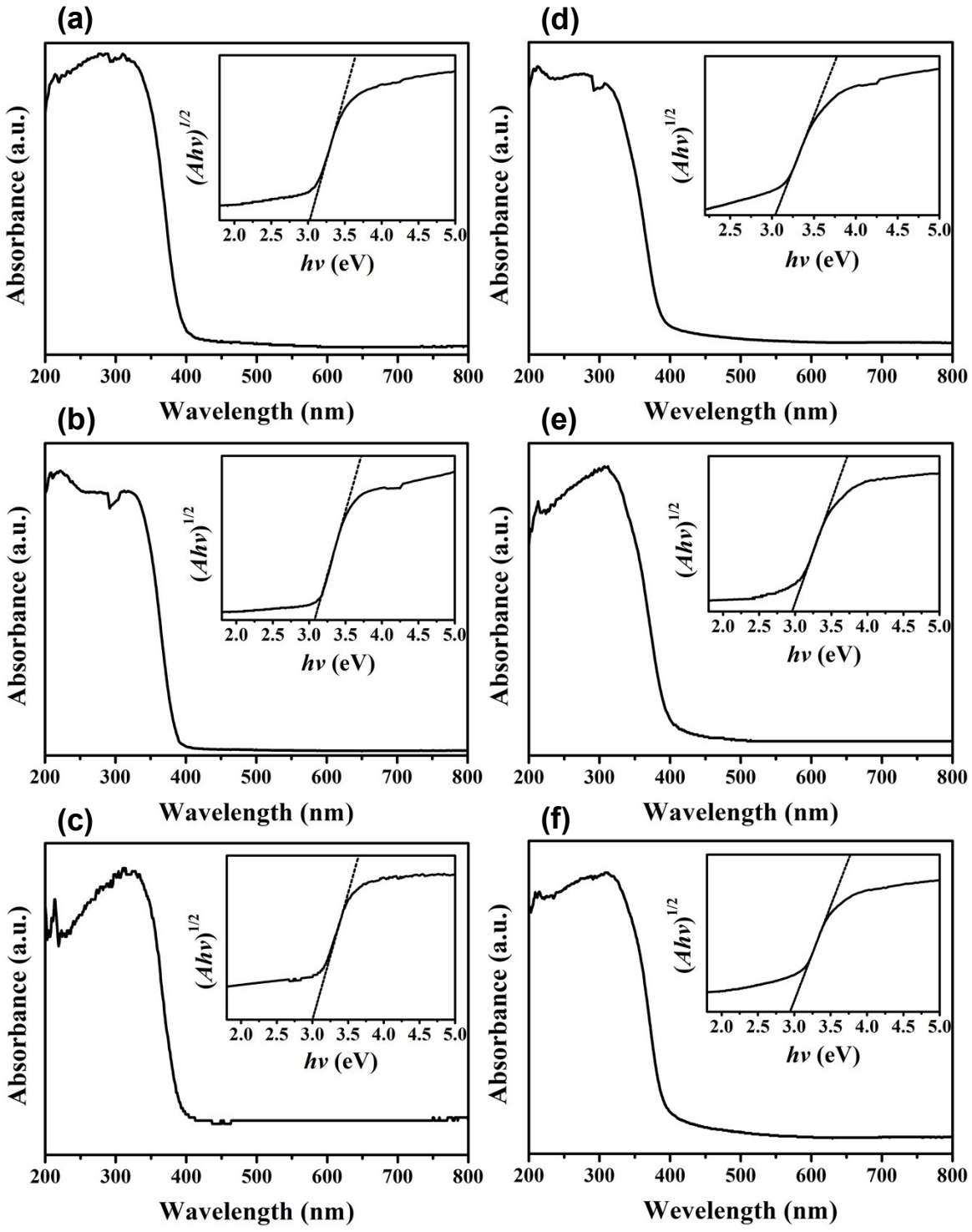

Fig. S4. UV-vis spectra of {101}_P (a), {101}_Air (b), {101}_Ar (c), {010}_P (d), {010}_Air (e), {010}_Ar (f) materials. Insets are the Tauc plots of the materials.

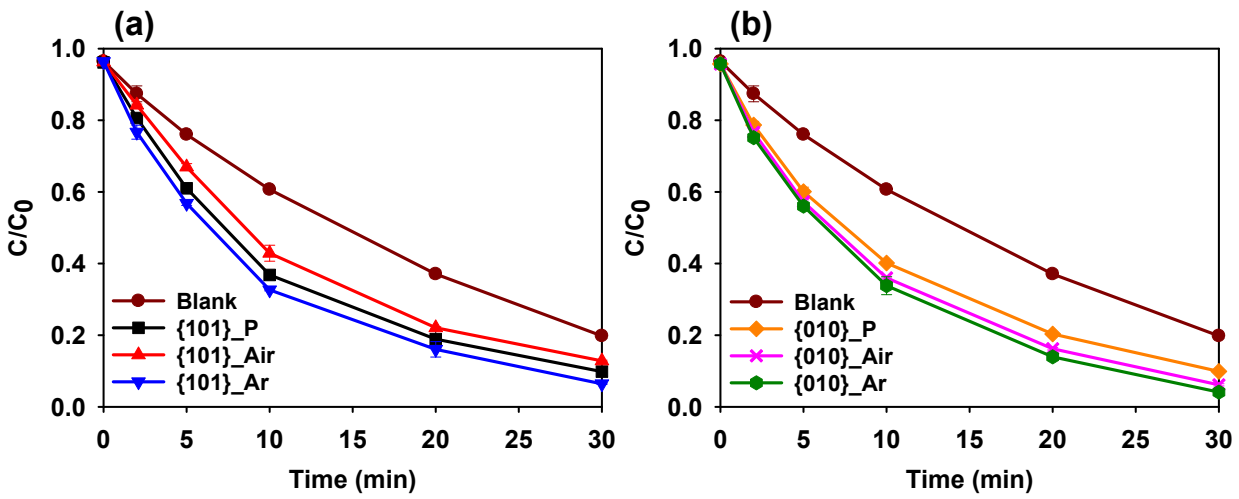

Fig. S5. Photocatalytic degradation of BPA by TiO_2 materials with predominantly exposed {101} facets (a) and {010} facets (b). Error bars represent the standard deviations (SD) of triplicate samples.

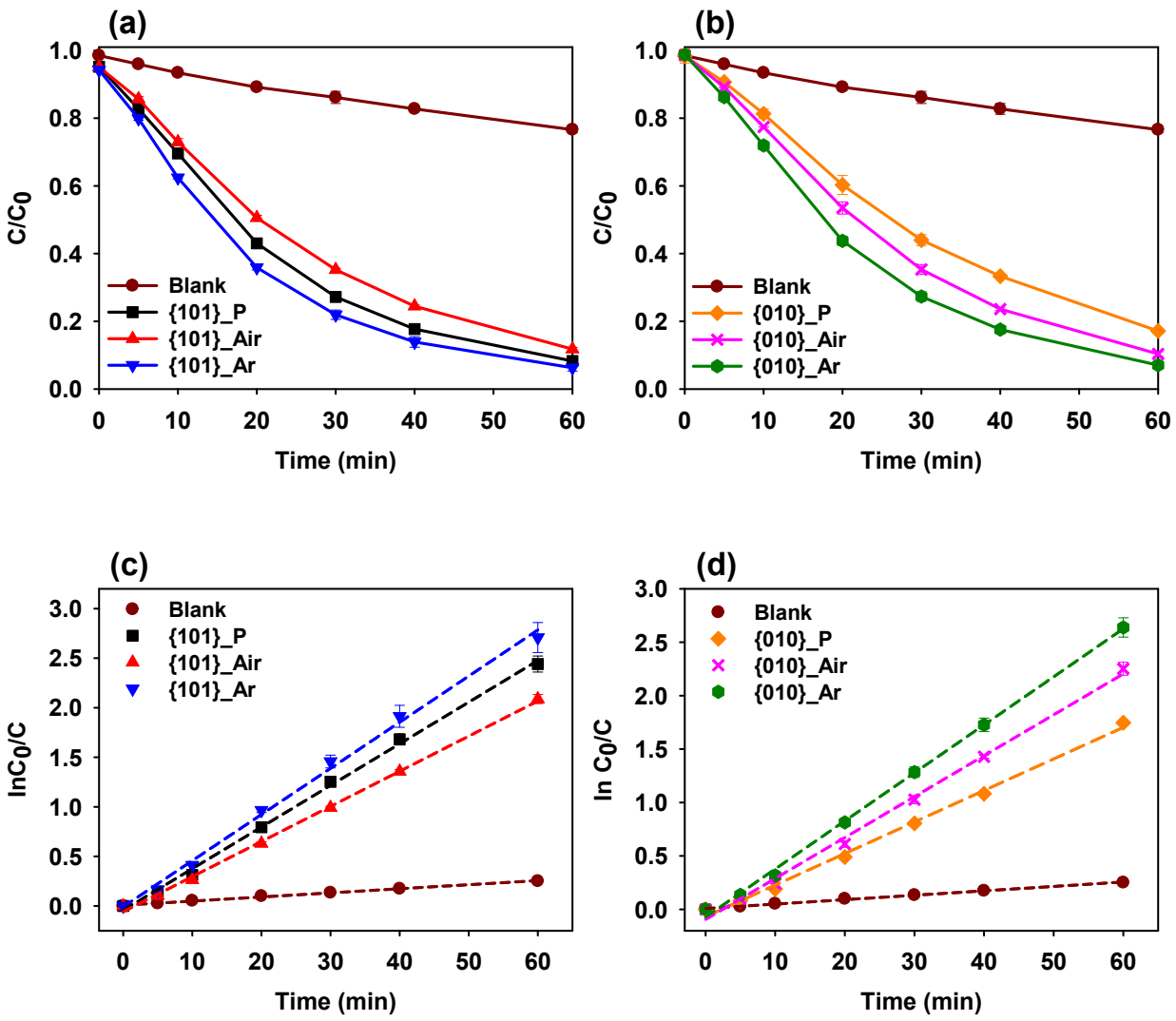

Fig. S6. (a, b) Photocatalytic degradation of RhB by TiO_2 materials with predominantly exposed {101} facets (a) and {010} facets (b), and (c,d) the corresponding degradation kinetics curves fitted to pseudo-first-order rate law. Error bars represent the SD of triplicate samples.

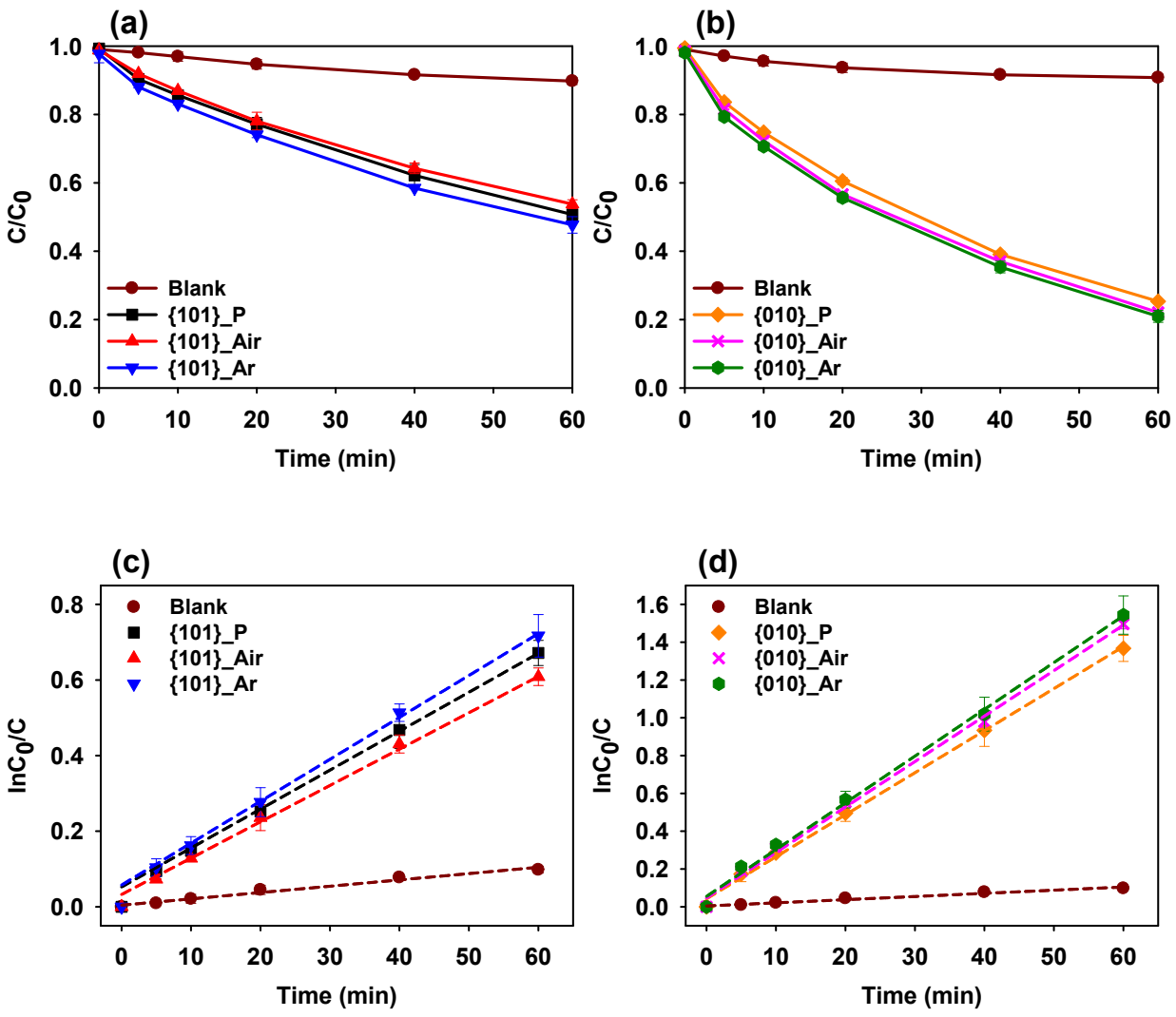

Fig. S7. (a, b) Photocatalytic reduction of Cr(VI) by TiO_2 materials with predominantly exposed {101} facets (a) and {010} facets (b), and (c,d) the corresponding degradation kinetics curves fitted to pseudo-first-order rate law. Error bars represent the SD of triplicate samples.

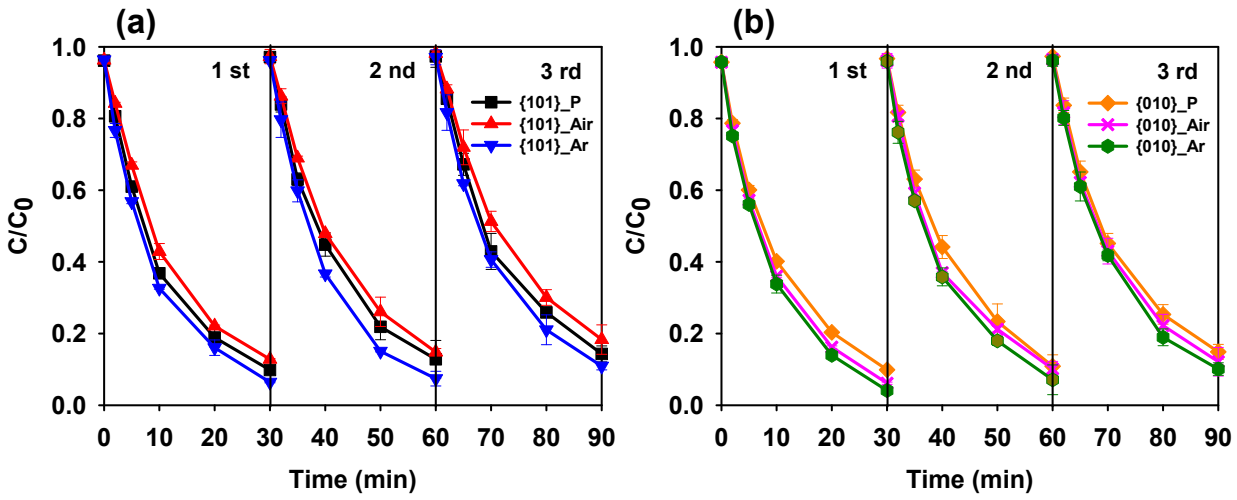

Fig. S8. Recycling photocatalytic degradation of BPA by TiO_2 materials with predominantly exposed {101} facets (a) and {010} facets (b). Error bars represent the SD of triplicate samples.

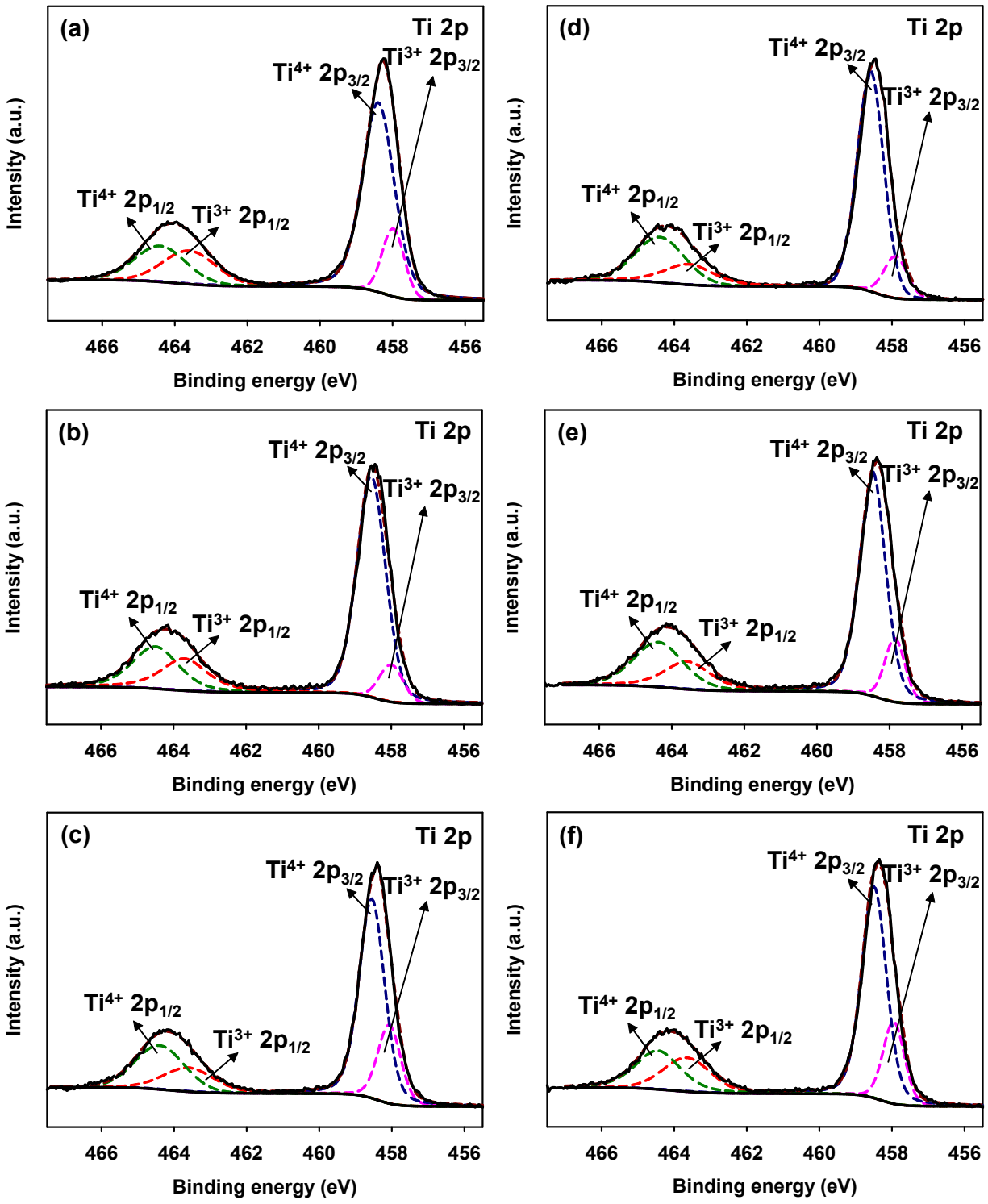

Fig. S9. High-resolution Ti 2p XPS spectra of {101}_P (a), {101}_Air (b), {101}_Ar (c), {010}_P (d), {010}_Air (e), {010}_Ar (f) materials after photocatalytic BPA degradation reactions.